

Modified Circumpolar Deep Water intrusions in Vincennes Bay, East Antarctica.

N. Ribeiro¹, L. Herraiz-Borreguero², S. Rintoul², C. R. McMahon³, M. Hindell¹, R. Harcourt⁴, G. Williams¹

¹Institute for Marine and Antarctic Studies, University of Tasmania, Hobart, Tasmania 7004, Australia.

²Commonwealth Scientific and Industrial Research Organization Oceans and Atmosphere, Hobart, Tasmania 7004, Australia.

³IMOS Animal Tagging, Sydney Institute for Marine Science, Sydney, 2000, Australia

⁴Department of Biological Sciences, Macquarie University, Sydney, New South Wales 2109, Australia.

Key Points:

- Oceanography of the Vincennes Bay shelf region and surrounds in late summer to early fall/autumn
- Widespread modified Circumpolar Deep Water in Vincennes Bay and basal-melt of local glaciers
- Vincennes Bay Bottom Water production susceptible to increasing glacial melt-water input

Corresponding author: Natalia Ribeiro, natalia.ribeirosantos@utas.edu.au

Abstract

Antarctic Bottom Water (AABW) production supplies the deep limb of the global overturning circulation and ventilates the deep ocean. While the Weddell and Ross Seas are recognised as key sites for AABW production, additional sources have been discovered in coastal polynya regions around East Antarctica, Vincennes Bay being the latest. Vincennes Bay, despite encompassing two distinct polynya regions, is considered the weakest source, producing Dense Shelf Water (DSW) only just dense enough to contribute to the lighter density classes of AABW found offshore. Importantly, the network of local glaciers and upstream Totten Ice Shelf system are all reportedly thinning and the freshwater input from such melting is likely to influence water mass structure. Accordingly, Vincennes Bay presents an interesting test case for DSW/AABW sensitivity to climate-driven changes in Antarctic coastal oceanography. Here we provide the first detailed observations of the Vincennes Bay shelf region and surrounds, using CTD data from instrumented elephant seals in late summer/early fall. We find that Vincennes Bay has East Antarctica's warmest recorded intrusions of modified Circumpolar Deep Water (mCDW), intrusions that both hinder sea-ice production and contribute salt to new DSW formation. Warm mCDW is also observed to be driving basal melt in Vincennes Bay, as seal CTD data provide the first direct observational evidence for inflow of basal melt to this region. As the most marginal of AABW sources, Vincennes Bay is a particularly useful region for assessment of the sensitivity of AABW production to changes in climate.

Plain Language Summary

The production of Antarctic Bottom Water (AABW), the densest water in the ocean, is a key factor of the global ocean circulation, distributing heat and helping to regulate the climate. The formation of AABW is dependent on the sea-ice production of some coastal polynyas around Antarctica, among those, the ones located in Vincennes Bay. The study shows that relatively warm water that is normally offshore is coming onto the continental shelf in Vincennes Bay, threatening the balance of this system by making the waters warmer and making it difficult for the polynyas to form sea ice. The warm intrusions are the warmest observed in East Antarctica and are also causing the melt of the local glaciers. The resulting input of freshwater makes the local waters less salty and forces this warm water to deeper levels, where it can do more damage to the local ice shelves. Our findings indicate that Vincennes Bay AABW is lighter than in other source regions, because it is already being affected by the warm water intrusions. It is important to keep investigating Vincennes Bay, since it is the AABW source that is likely to shut-down first.

1 Introduction

The production of Antarctic Bottom Water (AABW) is a key part of the global overturning circulation, transporting gases to the bottom of the ocean basins (Marshall & Speer, 2012). Historically the large continental ice shelves and embayments of the Weddell Sea (Gill, 1973) and Ross Sea (Jacobs et al., 1970) have been considered the most important regions for the production of AABW. More recently, new source regions of Dense Shelf Water (DSW) have been discovered in East Antarctic coastal polynyas, including the Mertz Glacier in Adélie Land (Rintoul, 1985; Williams et al., 2010, 2008), Cape Darnley/Prydz Bay (Ohshima et al., 2013; Williams et al., 2016) and most recently Vincennes Bay (Kitade et al., 2014). In each location, the potential to form and export DSW depends on a combination of factors, including the amount of brine released by sea-ice formation in coastal polynyas, freshening by ice-sheet melt, cross-shelf and along-shelf exchange, and steering of currents by coastal bathymetry. Despite many observational and modelling studies of the formation and transport of AABW, estimates of the total volume transport remain uncertain (Jacobs, 2004).

The finding of each new polynya source of AABW in East Antarctica has redefined the existing paradigm. In establishing that, out of the many polynyas around East Antarctica, only the Mertz Glacier polynya could potentially produce as much AABW as the Ross Sea, the large storage volume of the Adélie Depression was thought to be a crucial factor as it allowed salinity to build through the winter sea-ice growth season (Bindoff et al., 2001; Williams & Bindoff, 2003). Similarly, when the Cape Darnley polynya was discovered to have some of the highest DSW salinities in all Antarctica, yet lacked storage volume on the continental shelf, it was first linked to the sheer intensity of the Cape Darnley polynya (Ohshima et al., 2013) and then additionally to the upstream ‘pre-conditioning’ from a less saline variant of DSW from Prydz Bay (Williams et al., 2016). While Prydz Bay has an equivalent amount of polynya activity as Cape Darnley (Williams et al., 2016), the salinity of its DSW is suppressed by the freshening impact of meltwater from the Amery Ice Shelf (Herraiz-Borreguero et al., 2015; Williams et al., 2016). This was the first observational evidence of the potential for enhanced/accelerating melting of Antarctica’s ice shelves to threaten AABW production.

The discovery of the AABW formation in Vincennes Bay at 110°E (Fig. 1) was somewhat unexpected, given the relatively modest sea-ice formation in its polynya, its narrow continental shelf and absence of upstream polynyas (Kitade et al., 2014). Indeed, this AABW source was found to be relatively weak and likely to contribute only to the upper levels of the offshore AABW (Kitade et al., 2014). Nonetheless, it may be an important local source region to consider for two reasons. First, as a ‘weak’ source of AABW it provides an example of a bottom water source that is delicately poised and therefore likely to be sensitive to change. Second, the region is downstream of a large source of freshwater, the Totten Glacier system, and has a number of local glacial sources.

The Totten Glacier is the major outflow region for the Aurora basin and has been thinning and losing mass in recent decades (Velicogna et al., 2014). The glacier is reportedly already experiencing a positive feedback in which inflow of warm water at depth drives more basal melt, and more melt increases stratification, inhibits DSW formation, and enhances warm inflow driving further melt (Silvano et al., 2017, 2018). As mentioned, several glaciers feed into Vincennes Bay, the two largest being the Underwood and Vanderford glaciers. These are also outflow gateways for the Aurora basin and too have been thinning and losing mass in recent decades, albeit at a lower rate than the Totten Glacier (Witze, 2018; Velicogna et al., 2014). Significantly, the physical processes underlying their thinning are currently unknown.

We examine the oceanography of the Vincennes Bay shelf region and surrounds using CTD data from instrumented seals. In particular, we detail the pathways and properties of the mCDW intrusions in this region relative to the areas of polynya activity, with the aim of assessing: (i) the impact on the basal melting of the local glaciers and, (ii) the factors that regulate the capacity of this region to produce Antarctic Bottom Water.

2 Data and Methods

2.1 Study Area

Our study area is centred on Vincennes Bay, defined as the shelf region from 104° to 111°E situated between Cape Nutt and Cape Folger along the Knox and Budd Coasts of Wilkes Land, East Antarctica (Fig. 1). Vincennes Bay has several outlet glaciers, with the Vanderford and Adams glaciers on the eastern flank and the Bond and Underwood glaciers on the western side (Fig. 1a). Historically, the Vincennes Bay Polynya has been defined as the polynya region adjacent to the Vanderford Glacier on the eastern flank of the bay, but the foraging behaviour of the seals provides access to data from a smaller polynya region west of the Underwood Ice Shelf (Fig. 1b). Accordingly, we will consider

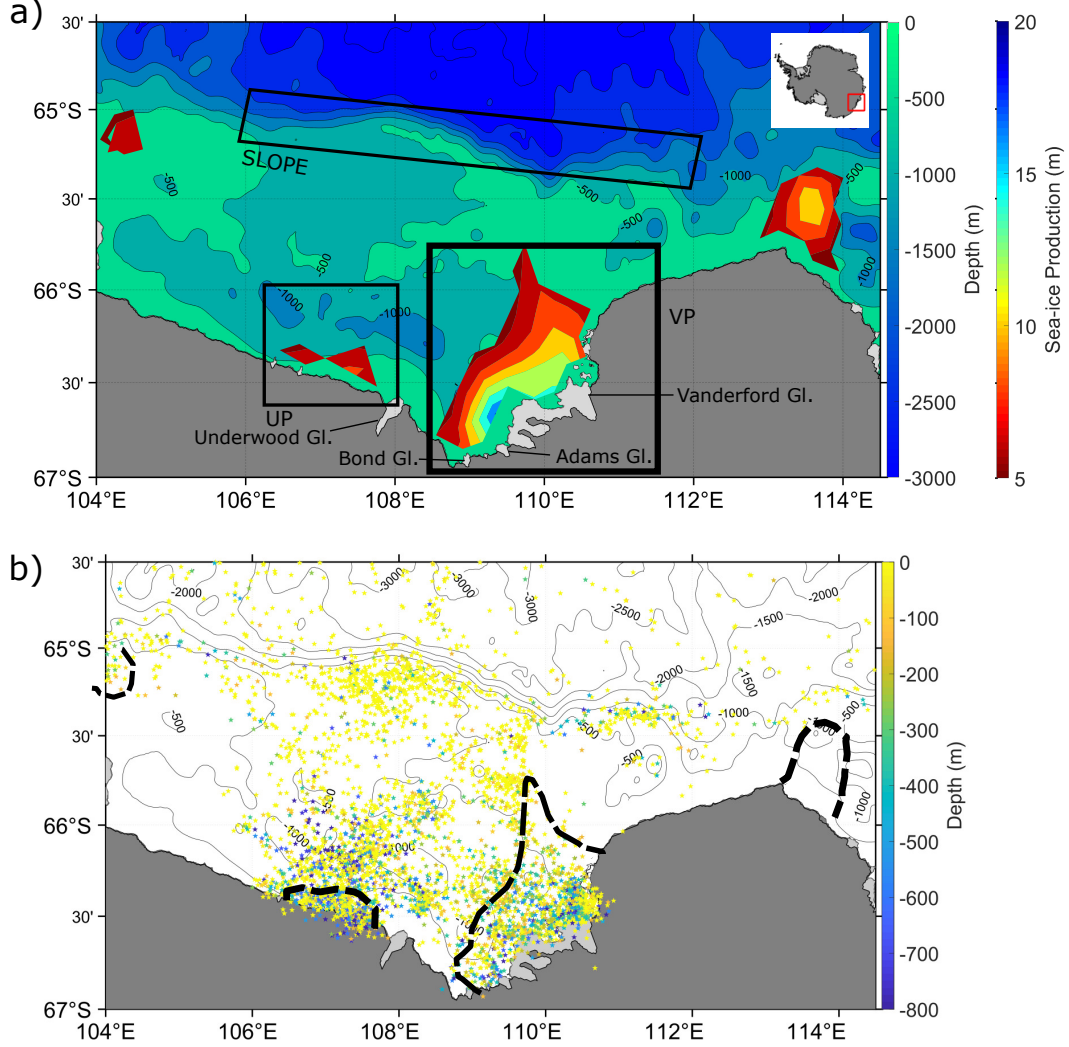


Figure 1. Region of Study and Data Distribution. **a)** The map shows Vincennes Bay and the subdivided regions used in this study (black rectangles). Sea-ice production contours are an average of 10 years (2008-2017) of satellite data, provided by Dr. Takeshi Tamura. **b)** Seal CTD data distribution showing the difference between seal dive depths and the known bathymetry of the area. The black dashed lines indicates the boundary of the two coastal polynyas in the region. Bathymetry, coastline and ice shelves are from Bedmap2 (Fretwell et al., 2013).

both polynya regions, the Vanderford Polynya (VP) to the east and the Underwood Polynya (UP) to the west.

Three sub-regions are defined to assist in the analysis of Vincennes Bay oceanography, based on the availability of seal data. The ‘slope’ region (Fig. 1b) encapsulates the shelf break and upper continental slope north of Vincennes Bay where the water masses from the Southern Ocean enter and water masses transformed by shelf processes depart. The remaining two subregions encompass Vanderford and Underwood polynyas of Vincennes Bay.

2.2 Oceanographic data and water masses

2.2.1 Instrumented seal CTD data

The oceanographic data (salinity, temperature and depth) used in this study comes from instrumented southern elephant seals (*Mirounga leonina*; CTD-SRDL) downloaded from the Marine Mammals Exploring the Ocean Pole to Pole (MEOP) Consortium website (www.meop.net). Seal CTD-SRDL data have helped fill gaps in sampling of Antarctic regions where data from ships are limited due to sea ice or challenging weather conditions (Roquet et al., 2014; Williams et al., 2016; Treasure et al., 2017; Harcourt et al., 2019). In total 5396 CTD profiles are available in Vincennes Bay from 2012, when 22 seals were tagged at Casey Station (110.53°E). The data covers most of the year from February to November, with the highest number of profiles returned between February and May.

The CTD-SRDLs record the ascending profiles at 1Hz sampling frequency, retaining only the deepest dive within a six-hour period. The location of the individual profiles is provided by the Advanced Research and Global Observation Satellite (ARGOS) system, precise to within a few kilometres using the data processing method described in Roquet et al. (2017). While CTD-SRDL data is less accurate than ship-based measurements, there has been ongoing development of the post-processing protocols (Siegelman et al., 2019; Mensah et al., 2018; Jonsen et al., 2020). The final accuracy of the salinity and temperature data is estimated to be ≈ 0.03 and $\approx 0.03^\circ\text{C}$, respectively (Siegelman et al., 2019).

2.2.2 Antarctic Water Mass Definitions

There is some variability in the nomenclature and properties used to define water masses around the coastal margin of Antarctica, especially in regions of Antarctic Bottom Water production (Jacobs et al., 1970; Williams et al., 2016; Kitade et al., 2014). We follow the water mass definitions of Williams et al. (2016) and Silvano et al. (2017) (with minor adjustments to account for the reduced salinity of the region), initially using neutral density to distinguish the three classic offshore water masses of Antarctic Surface Water (AASW), CDW and AABW (Tab. 1). Water mass transformations driven by ice-ocean-atmosphere interactions over the continental shelf produce three additional water masses: Winter Water (WW), DSW and Ice Shelf Water (ISW).

Over the continental slope, fresh and cool AASW incorporate both the winter and summer mixed layers. WW is the name given to the winter mixed layer within the AASW. The denser CDW is ‘modified’ (cooled and freshened) as it moves southwards and intrudes across the continental shelf break in discrete locations, where it is referred to as modified CDW (mCDW). If sea-ice formation is weak, then the mCDW will be bottom-intensified below the winter mixed layer of the AASW. However, if the sea-ice formation is intense, as in large coastal polynyas, then the winter mixed layer will convect to the bottom and form DSW, the pre-cursor to AABW. In regions where DSW is formed, the lighter mCDW will intrude on the continental shelf at mid-depth, rather than near the seabed (Narayanan et al., 2019; Williams et al., 2010, 2008).

Table 1. Classification of the Water Masses

Water Mass	$\gamma^n(kgm^{-3})$	$\theta(^{\circ})$	Salinity
AASW	$\gamma^n < 28$		
CDW	$28 < \gamma^n < 28.27$	$\theta > 1.5$	
mCDW	$28 < \gamma^n < 28.27$	$1.5 < \theta < -1.7$	
WW	$27.55 < \gamma^n < 27.7$	$\theta < -1.8$	
DSW	$\gamma^n > 28.27$	$-1.92 < \theta < -1.8$	$S > 34.4$
ISW		$\theta < -1.92$	

Given the physical properties of sea water and how its freezing point responds to pressure (Foldvik & Kvinge, 1974), all shelf water masses (AASW, mCDW, DSW) can melt ice shelves at different depths. A typical cold cavity ice shelf has, in general, lower area-averaged rates of basal melt than a warm cavity ice shelf (e.g., Silvano et al., 2016). The Mertz Glacier Tongue and Amery Ice Shelf are cold cavity ice shelves in East Antarctica, with area-averaged melt rates less than 2 myr^{-1} (Rignot et al., 2013; Liu et al., 2015). Melt rates in warm cavity ice shelves can vary from 4 to 20 myr^{-1} per area-averaged (Rignot et al., 2013; Liu et al., 2015).

Depression of the freezing temperature with pressure means that large glacial melt rates occur at depth. Thus, the strongest melt typically occurs at the grounding line, driven by the densest water mass (mCDW or DSW) present in the region. The buoyant meltwater rises along the sloping base of the ice shelf, all the while mixing with ambient waters. The mixture of glacial meltwater and ambient waters can form ISW, which has a temperature below the surface freezing point. For ISW to form, deep grounding lines and cold cavities are necessary. Glacial meltwater, either as ISW or not, can also be detected using isotopes of oxygen and the noble gas Helium (Schlosser et al., 1991).

3 Results

3.1 Distribution of Water Masses in Vincennes Bay

We begin by examining the distribution of key water masses (as defined in Table 1) on the continental shelf of Vincennes Bay during late summer/autumn (Fig. 2). The dominant water mass both on and off the shelf is the warm and relatively saline mCDW (Fig. 2a). The Antarctic Slope Front (ASF) is the boundary between warm offshore CDW and colder shelf waters, traditionally defined using the position of the subsurface 0°C isotherm (e.g., Jacobs, 1986, 1991). The seal CTD data, primarily from March through April, shows that the subsurface 0°C isotherm is well south of the shelf break between 108° and 110°E (Fig. 2a). As the 0°C isotherm is commonly used to describe the presence, strength and variability of mCDW intrusions around the Antarctic shelf break, this is an indication that in Vincennes Bay mCDW intrusions are not only present but quite strong.

The maximum mCDW temperature at the inner shelf break is centred around 109°E . At around 65.5°S , the inflow of CDW appears to bifurcate across the central shelf area (Fig. 2a), cooling on its way to the coast. Here, maximum temperatures of $\approx 0.5^{\circ}\text{C}$ are recorded at the northern flank of the Vanderford Glacier, within the Vanderford polynya

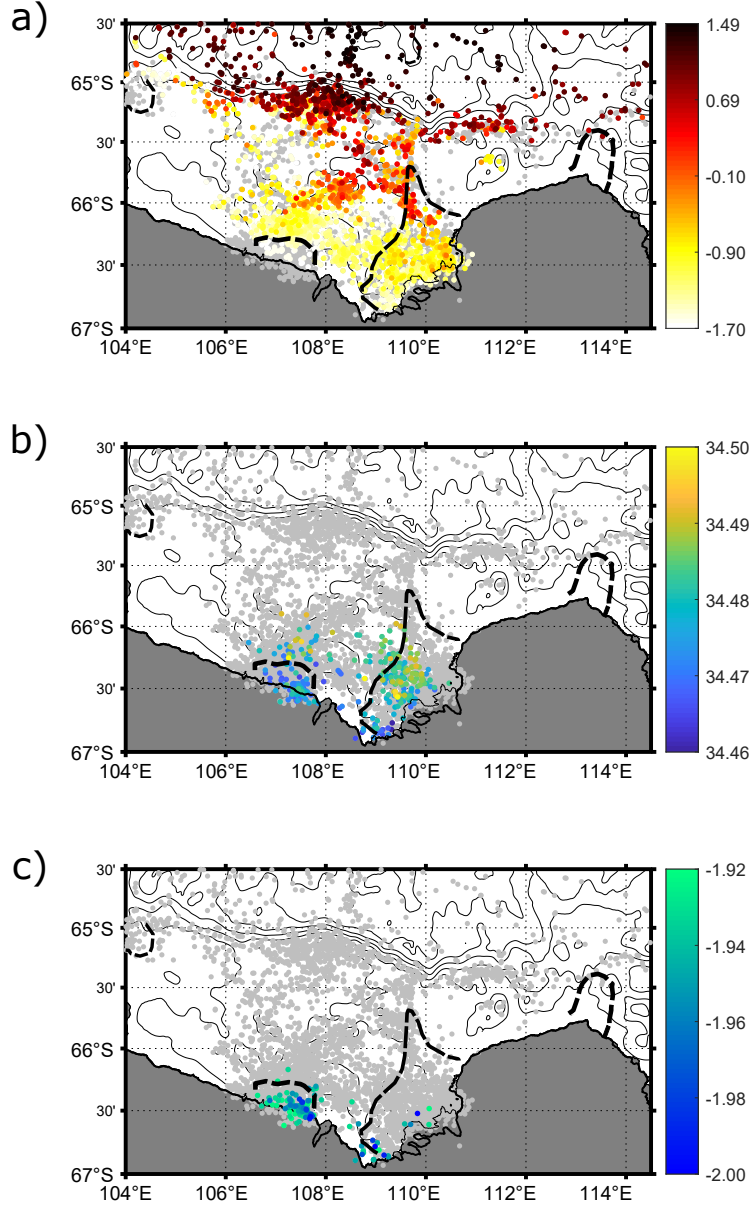


Figure 2. Water Mass Distribution (a) mCDW. Intrusions of mCDW are signalled by maximum temperature values (θ_{max} °C) across the platform, predominantly to the East. (b) DSW. Maximum salinity values are associated with the production of DSW by polynyas. The actual maximum value was 34.57, but second highest is displayed for scale purposes. (c) ISW. Minimum potential temperature (θ_{min} °C) indicates a cold coastal signal to the west ($\theta_{min} < -1.92$). Sea-ice contours are an average of 2008-2017 years, data provided by Dr. Takeshi Tamura (dashed-black lines).

(Section 3.3). The scale and magnitude of these mCDW intrusions is quite remarkable compared to other East Antarctic regions, but on par with the Totten Glacier/Sabrina coast region directly upstream (Silvano et al., 2017, 2018). In the water column, the seals recorded the warmest mCDW between 200 and 900 dbar (or near the bottom depending on the bathymetry; Section 3.3).

Next we consider Dense Shelf Water and Ice Shelf Water in the context of the two polynya regions and local glaciers/ice shelves. DSW is primarily found in the Vanderford Polynya, and to a lesser extent in the Underwood Polynya region to the west (Fig. 2b). Mean salinity for these DSW was 34.49 with a maximum salinity of 34.52, which is right at the lower bound for DSW ($\gamma^n > 28.27$) around Antarctica (Williams et al., 2016; Kitade et al., 2014). Given these are late summer/autumn observations, this DSW is remnant from the previous winter's sea-ice growth season. There is also evidence of remnant DSW in small troughs within the shelf (Fig. 2b).

ISW is the result of glacial meltwater mixed with ambient water masses and so its properties can vary seasonally. Using temperature alone to distinguish glacier meltwater is problematic if the source is weak and the supercooled temperature signal is quickly eroded through mixing in the ice-shelf cavity. Nonetheless Figure 2c shows the signal of cold ISW ($\theta < -1.92^\circ\text{C}$) in the western flanks of the Vincennes Bay glaciers. The coldest ISW (-2.05°C) is found immediately adjacent to the western Underwood Glacier ice-shelf front. The depth at which ISW was observed ranged between 350 and 600 dbars, suggesting that the ice-shelf fronts are at least 350m thick. The observations of ISW are not unexpected given the strong inflow of oceanic heat into Vincennes Bay. Yet, this is the first direct observational evidence for inflow of basal melt to this region. We also observed the presence of meltwater plumes within the water column that do not classify as ISW (shown in Section 3.3). We assume that ISW is mixing with these plumes and losing its sub-freezing point temperature signal, as observed in the Totten region (Silvano et al., 2017, 2018).

3.2 Cross-shelf exchange of mCDW into Vincennes Bay

Given its dominant presence and likely impact on local glacial melt and dense shelf water formation, we now examine the cross-shelf exchange of mCDW into Vincennes Bay and its subsequent pathway towards the polynyas in more detail. Sections of potential temperature and salinity along the continental shelf break are shown in Figure 3a-b. The warmest CDW (1.42°C) is observed between 108° and 110° E (Fig. 3a-b).

mCDW is present along the entire slope, filling the water column below $\gamma^n=28$ (200-400 dbars to the bottom) with a core temperature of 1.4°C and a salinity of 34.8 (Fig. 3a-b). The $\gamma^n=28$ marks the upper limit of mCDW, which deepens from 200 to 400 dbars between April and June, following the formation of the winter mixed layer (Section 3.3). The eastern part of the slope, between 0 and 400m, is dominated by a homogenous layer of low salinity (≈ 34.2) that might indicate a potential input of freshwater onto the shelf from neighbouring glaciers.

We estimate the total transport across this region (Fig. 3c) and specifically the temperature transport associated with the mCDW layer (Fig. 3d). Geostrophic velocity (V_g) and volume transport across the continental shelf break was estimated using the thermal wind relation and a reference level at the sea surface. Temperature transport was calculated by multiplying the geostrophic velocity by temperature (K Sv) and integrating over the area of the section (Eq. 1).

$$T_r = \int \int \theta V_g dx dz \quad (1)$$

The mCDW intrusions are strongest through the central-west part of the slope and accordingly the temperature transport increases to the west, reaching -1.4×10^7 K Sv at

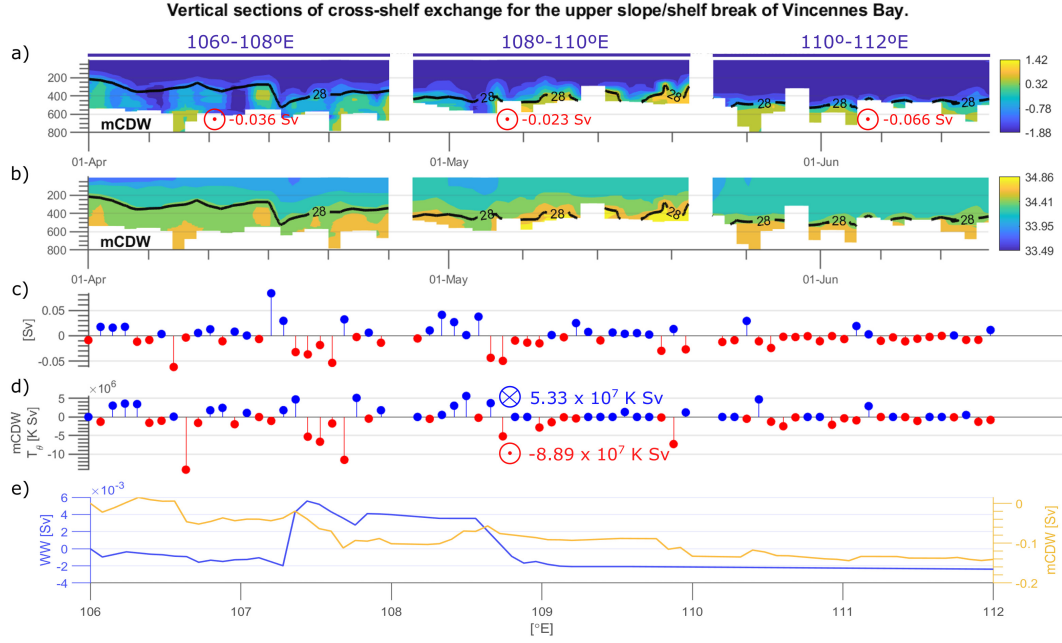


Figure 3. Cross-shelf exchange for the upper slope/shelf break of Vincennes Bay
 Shown are geographically and time-spaced vertical sections of a) potential temperature (°C) and (b) salinity. Total transport and direction per section is shown in red. c) Net transport calculation (Sv) with a 0.25° resolution for the cross-shelf: transport southwards is in red and northwards is shown in blue. d) Temperature transport (K Sv) associated to mCDW profiles: southwards in red and northwards in blue. e) Cumulative transport (Sv) from west to east for WW (blue) and mCDW (yellow).

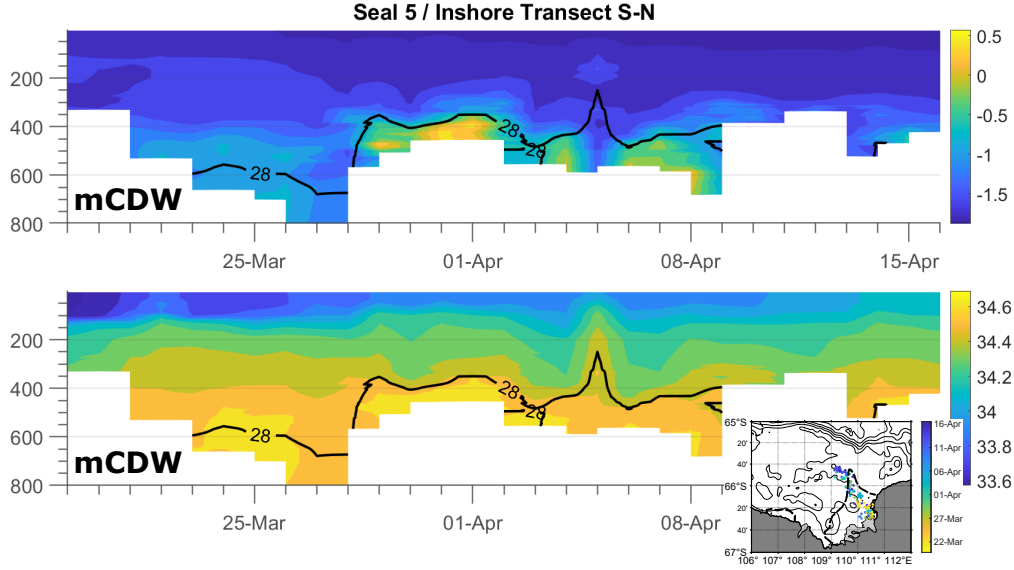


Figure 4. Across shelf penetration of bottom-intensified mCDW. Vertical sections of a) Potential temperature and b) Salinity compiled from Seal 5 CTD data between 22nd Mar and 16th April. Inset: Location of data with date

$\approx 106^\circ\text{E}$ (Fig. 3d). The western side of Vincennes Bay is significantly deeper and likely facilitates spread of mCDW through the entire shelf. Overall, there is a total net temperature transport of $3.56 \times 10^7 \text{ K Sv}$ onto the shelf (8.89 and $5.33 \times 10^7 \text{ K Sv}$ going south/north).

To better visualize the contributions of each water mass on the transport across the slope, Figure 3e shows the cumulative transport for mCDW (yellow) and for WW (blue) from west to east. While the main volume transport into Vincennes Bay comes from the mCDW intrusions between 300-600 m, there is also fresher WW (≈ 34.2 at 0–400m, Fig. 3b) coming in (Fig. 3e). It comes in on and off along the slope, but more consistently from the east (110 - 112°E). The WW transport observed across the Vincennes Bay slope has a salinity range of 33.92-34.3.

Getting across the upper slope/shelf break region is the first hurdle that a mCDW intrusion must negotiate. Thereafter, its continued progress/mixing towards the coast is dictated by bathymetry and its properties/buoyancy relative to the ambient shelf waters. We now examine this process for Vincennes Bay by virtue of Seal 5's foraging strategy between 22nd March and the 16th April, which facilitated a vertical section north-westward from the Vanderford Glacier to the central shelf region at 109.5°E (Fig. 4, inset). This section captures the core of a significant mCDW intrusion up to 300m thick (Fig. 4). The most significant feature, beyond its temperature maximum of 0.5°C , is that this mCDW is bottom-intensified. That is, in spite of its warm temperature, mCDW is the densest water mass on the continental shelf in the areas where no DSW is present. The relative position of mCDW heat and salt supply in the water column has important consequences for both polynya activity and glacier/ice-shelf melting.

3.3 Winter mixed layer formation

Polynyas are sea-ice factories. The efficacy with which polynyas produce dense shelf waters can be negatively impacted by several processes, including the grounding of icebergs in the vicinity of the polynyas affecting import and export of sea ice (e.g. in the Mertz, Kusahara et al., 2010) and freshwater inputs from ice-shelf melting (Silvano et

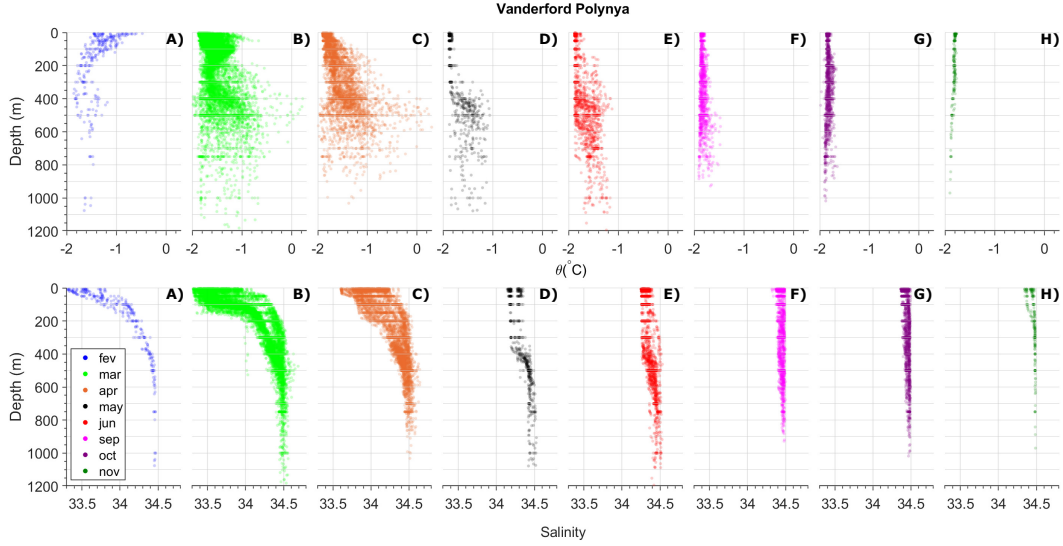


Figure 5. Winter mixed layer evolution in Vanderford Polynya. First panel shows the potential temperature vertical profiles and the second panel the salinity profiles for all months available.

al., 2017). The coverage of Vincennes Bay by the instrumented seals makes it possible to study the evolution of the winter mixed layer and thus, the formation of DSW, within the polynyas. The evolution of the winter mixed layer formation in the Vanderford and Underwood polynyas are shown in Figures 5 and 6, respectively.

The VP struggles to form top-to-bottom winter mixed layers. Expected heat loss to the atmosphere from the ocean mixed layer is observed in both polynyas, resulting in cooling, salinification and deepening of the mixed layer throughout the winter months. By the end of the austral summer (March), relatively fresh summer mixed layers ($S < 34$) are observed in the top 200 dbars (Fig. 5, a and b). During April, an overall cooling and salinification of the mixed layer is observed, with no significant change in the depth of the mixed layer. Warm mCDW (of up to 0.5°C at around 500 dbar) and ISW are observed between 200 and 600 dbars up until May (Fig. 5b, c, and d). By May, the mixed layer has further cooled and increased in salinity to a depth of 400 dbar (Fig. 5d). The temperature of this mixed layer is very homogeneous (with the caveat that seals clustered near the Vanderford ice shelf front). mCDW is cooler in June, however its temperature is still relatively warm (up to -1.2°C) compared to previous winter studies within East Antarctica (e.g., Williams et al., 2008).

By September-October, the winter mixed layer is observed to reach the bottom (Fig. 5f and h). However, the temperature spans between -1.7°C and -1.89°C , and salinity spans between 34.28 and 34.5 psu above 700 dbar. The bottom layers of the water column are more homogenous in their thermohaline properties and a slow salinification is observed from June, reaching 34.6 psu by November (Fig. 5h and Fig. 7, first panel). It is worth mentioning that these profiles give us an overview of what happens within the polynya during active convection, and the differences in θ/S and depth of the winter mixed layer is also subject to spatial variability within the polynya (Fig. 8f).

Top-to-bottom convection is not observed in the Underwood Polynya (Fig. 6), but data are only available through June. If deep convection occurred later in the winter, as seen at Vanderford, it would not be captured by the seal data. The evolution of the winter mixed layer is similar to that observed in Vanderford polynya (Fig. 5 and 7). The

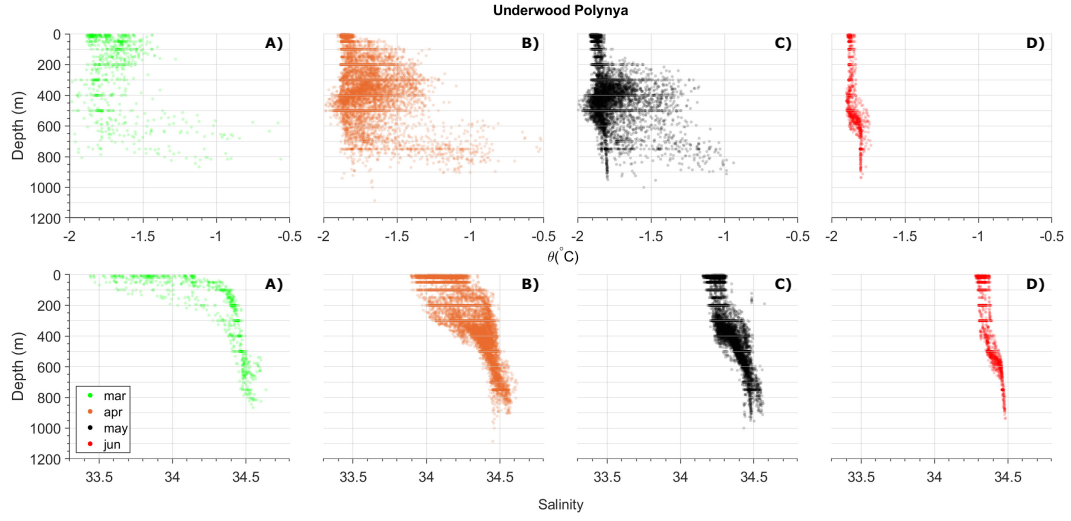


Figure 6. Winter mixed layer evolution in Underwood Polynya. First panel shows the potential temperature vertical profiles and the second panel the salinity profiles for all months available.

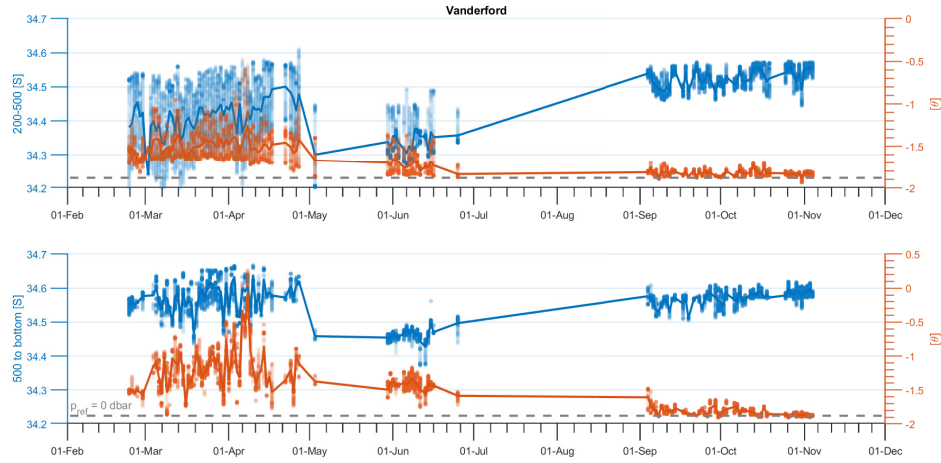


Figure 7. Potential Temperature and Salinity Time Series for VP. First panel shows the time series for the averaged potential temperature (orange) and salinity (blue) at 200-500 dbar. Second panel shows the time series for the averaged potential temperature (orange) and salinity (blue) from 500 dbar to the bottom.

main difference is where the warmest mCDW layer is located in the water column. While in the Vanderford polynya, the warmest mCDW ($\theta \approx -0.5^\circ\text{C}$) is observed between 400 and 600 dbars, in the Underwood polynya, mCDW ($\theta \approx [-1, -0.5]^\circ\text{C}$) occupies only the bottom layer below ≈ 500 dbars. ISW is also observed in this polynya during April and May (Fig. 6c and d, respectively). In fact, the depth of the winter mixed layer coincides with the depth at which we observe ISW and/or the top of the warmest mCDW in both polynyas. Another common feature between the polynyas is the wide range of thermohaline properties within the boundary between the bottom of the winter mixed layer and the ISW/warmest mCDW layers. We relate this feature to glacial meltwater and this will be addressed in the Discussion (Section 4).

Despite no observed top-to-bottom convection in the Underwood polynya, the thermohaline properties observed at the bottom of the water column correspond to those of DSW. The properties of this DSW are similar to those observed within the Vanderford polynya, and it is likely to have been formed the previous winter given that deep winter convection is unlikely to have occurred prior to June in either polynya (Fig. 5 and 6).

4 Discussion

Vincennes Bay along the Knox and Budd Coasts of Wilkes Land, East Antarctica, has gained attention in recent years as Antarctica's fifth, albeit weakest, source of Antarctic Bottom Water (Kitade et al., 2014). Its initial discovery was made from offshore moorings which detected a relatively low salinity variety of modified Shelf Water on the continental rise, contributing to the upper layer of AABW in the Australian-Antarctic Basin. This was attributed to DSW formation in the Vincennes Bay polynya system. Despite the growing interest in the oceanography of this region there have been no detailed oceanographic measurements on the continental shelf to further elucidate this connection. Using oceanographic profiles collected by seals, we found that warm and saline mCDW is widely distributed on the shelf, positioning Vincennes Bay as the shelf region with both the widest spatial distribution of mCDW and the warmest mCDW ever recorded in East Antarctica (Rintoul et al., 2016; Herraiz-Borreguero et al., 2015; Bindoff et al., 1999). Moreover, mCDW causes basal melt of the local ice shelves which in turn, interferes with the formation of DSW by the Vincennes Bay polynyas.

In Vincennes Bay, DSW formation is affected by the advection of mCDW into the polynya in two ways. By supplying salt at depth, mCDW can enhance the formation of DSW. By supplying heat, mCDW affects the formation of DSW both (i) positively, by maintaining an open polynya, and (ii) negatively, through melting of the local glaciers and hence increasing the supply of freshwater into the system. The addition of meltwater increases the stratification of the water column, which weakens the formation of DSW by preventing deep convection. Indeed, very few profiles were indicative of top-to-bottom deep convection (Fig. 5, September to November). However, a winter mixed layer was formed, reaching down to the depths at which ISW was observed between 400-700 dbar (Fig. 7, May onwards). Importantly for detecting freshwater input, we found that the winter pycnocline remained between 500 and 800 dbar in the Vanderford polynya until November (Fig. 7h). Typically it is at these depths that we interpret the additional glacial freshwater is mixed with mCDW, resembling the export of glacial meltwater observed in Pine Island Bay (e.g., Jacobs et al., 2011) and more closely, near the Totten glacier, upstream of Vincennes Bay.

Two water masses are likely to be responsible for the basal melt of the Vincennes Bay glaciers, DSW and mCDW. The melt-freeze line or Gade line (Gade, 1979) links the meltwater laden plumes of seawater, for example ISW, and its source water mass. The Gade line links the observed DSW ($S \approx 34.45$) with the ISW observed in the Vanderford polynya but not with the one observed in the Underwood polynya (Fig. 8). DSW with

similar thermohaline properties are observed in both polynyas at the bottom of the water column, so if DSW entered the ice-shelf cavities, ISW would have similar properties in both polynyas. Deviation from the melt-freeze line occurs when ISW mixes with water masses with different source water salinities, so it is possible that the ISW observed in the Underwood polynya has mixed with other water masses, such as mCDW or a cooler/fresher mCDW as a result of mixing with meltwater.

mCDW can enter the local ice shelves and drive previously undetected basal melt. The most significant evidence of meltwater linked to mCDW intrusion is observed in the winter mixed layer formation between March and June. During sea-ice formation, brine is rejected into the water column and so the ocean gains salinity with a corresponding continuous increase of salinity over the winter months (Charrassin et al., 2010). Satellite estimates of sea-ice production suggest that the Vincennes Bay polynyas form sea ice throughout the winter months (Fig. 8f). However, between April and May, we observed a freshening of ≈ 0.2 psu between 200 and 400 dbar (Fig. 7a and Fig. 5). The only source of freshwater must come from the basal melt of the local glaciers. No ISW is observed during this time. However, we do see a cooler and fresher mCDW, bounded by the melt-freeze mixing line (Fig. 8a and b), between 400 and 700 dbar (Fig. 5e). The addition of melted glacial freshwater in the water column may explain the wide range of θ/S observed within the halocline during the winter months (e.g., Figs. 5 and 6).

The Vanderford Polynya is not the only East Antarctic polynya where freshwater has negatively impacted the formation of DSW or where bottom-intensified mCDW has been observed. The Totten Glacier was the first region in East Antarctica to be identified with bottom-intensified mCDW (Rintoul et al., 2016) and thereafter, studies illustrated the relationship between mCDW and DSW (Silvano et al., 2018; Narayanan et al., 2019; Morrison et al., 2020). Silvano et al. (2018) show how the lack of DSW formation in the Dalton polynya allows bottom-intensified intrusions of mCDW to reach the Totten cavity downstream from the Dalton polynya. In addition, enhanced ice-shelf melt helps maintain the strong stratification that isolates inflowing mCDW from cooling by the atmosphere (Silvano et al., 2016, 2017, 2018).

The inflow of mCDW in Vincennes Bay differs from what may be expected because of some unique physical features. At the centre of the basin, Vincennes Bay has pods of DSW formation in sufficient volumes to cause mCDW intrusions to split into two limbs (Fig. 2b). Although that could indicate that where and when DSW is present in the bay there is no mCDW (Narayanan et al., 2019), the interplay in the polynyas suggests otherwise. Both DSW and mCDW were found to be accessing the local glacier cavities throughout 2012 causing melt. In the Totten Glacier, there is a clear bottom-intensified mCDW beneath a meltwater-laden upper layer. In Vincennes Bay, although the configuration is the same, mCDW is not confined to depth and can occupy the water column from the base of the summer mixed layer to the bottom (Figs. 5 and 6, March (b) and April (c)). The depths at which mCDW approaches the Vanderford Glacier are also quite remarkable. Figure 9 shows the depths of maximum mCDW temperature (bottom panel) and the maximum mCDW temperature for all profiles in the bay (top panel), excluding the slope. Although most of its core distribution seems to be around 300-600m, mCDW extends to depths of up to 1354m, right by the glacier edge, with maximum temperatures of -1.2°C . In the Totten, Silvano et al. (2017) shows mCDW with maximum temperatures of -0.4°C reaching the glacier to depths of 1100m which delivers sufficient heat to cause local melting. Likewise, we identify a profile near the northern tip of Vanderford Glacier with maximum temperatures of -0.7°C at 1132m depth (Fig. 9, red star) capable of causing sub-glacial melt.

Recent glaciological studies show that the four glaciers in Vincennes Bay have been losing mass, at similar rates as the Totten glacier (Witze, 2018). All these glaciers drain the Aurora basin, which holds up to 3.5 m of sea level rise equivalent. Maps of ice velocity and surface height elevation show that the glaciers in Vincennes Bay have lowered

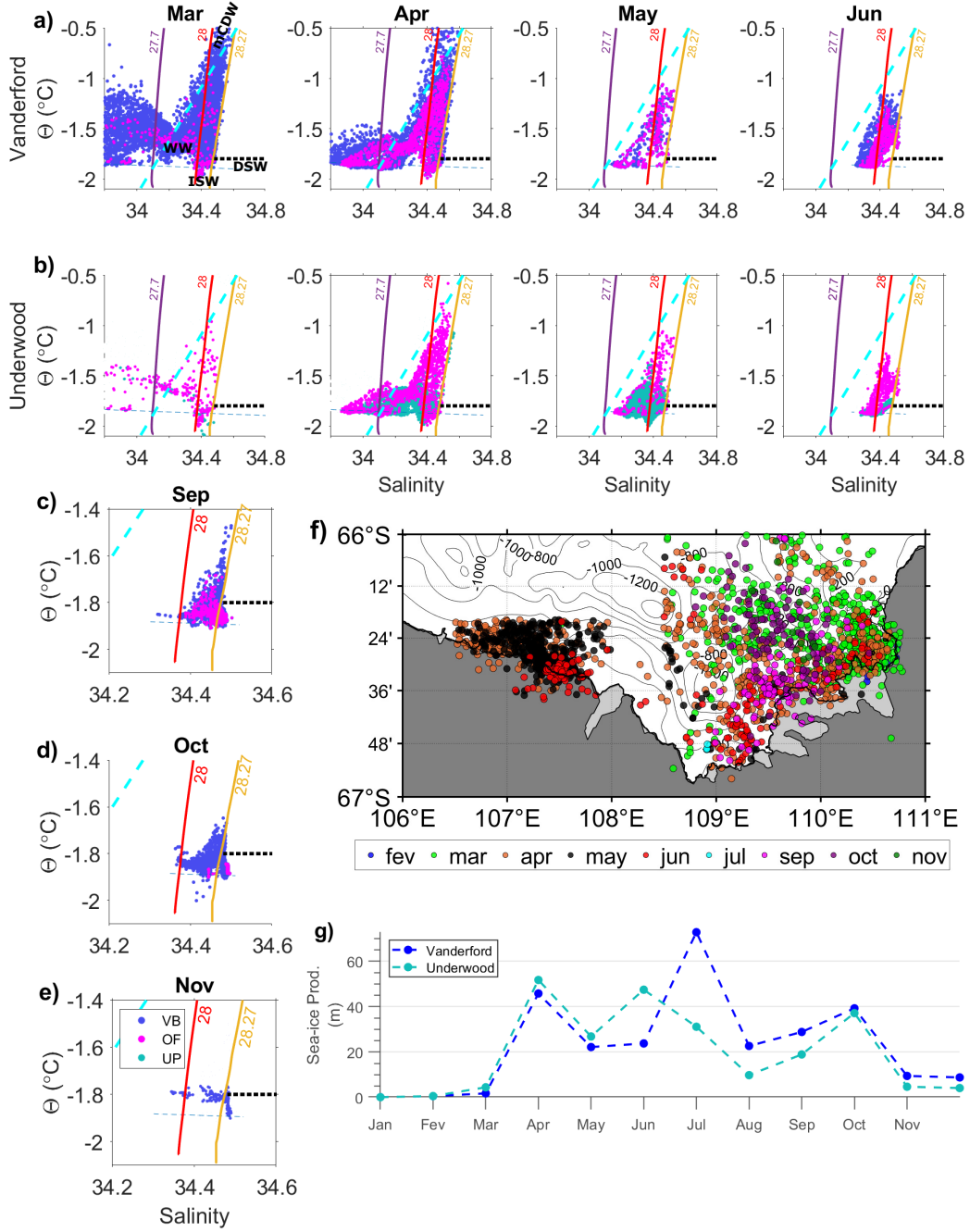


Figure 8. Vanderford vs Underwood. a) and b) TS distribution along Mar-Jun for VP (a, dark blue) and UP (b, green). c), d) and e) show additional months of data available in VP and its Outflow (OF), the region in between the two polynyas. The OF data points are plotted in pink over the data for both polynyas, firstly with VP data points (a) and then repeated again with the UP data points (b). The isopycnals of 27.7 (WW), 28 (mCDW) and 28.27 (DSW) are highlighted in purple, red and yellow, referring to a reference pressure of 0 dbar. Freezing point is shown by the blue dashed line and the mixing line (or Gade line) between the warmest mCDW found near the coast in VP polynya (-0.5°C) is shown in light blue dashed line. Monthly averaged SIP for 2012 is shown on the bottom panel in blue (VP) and green (UP), data provided by Dr. Takeshi Tamura.

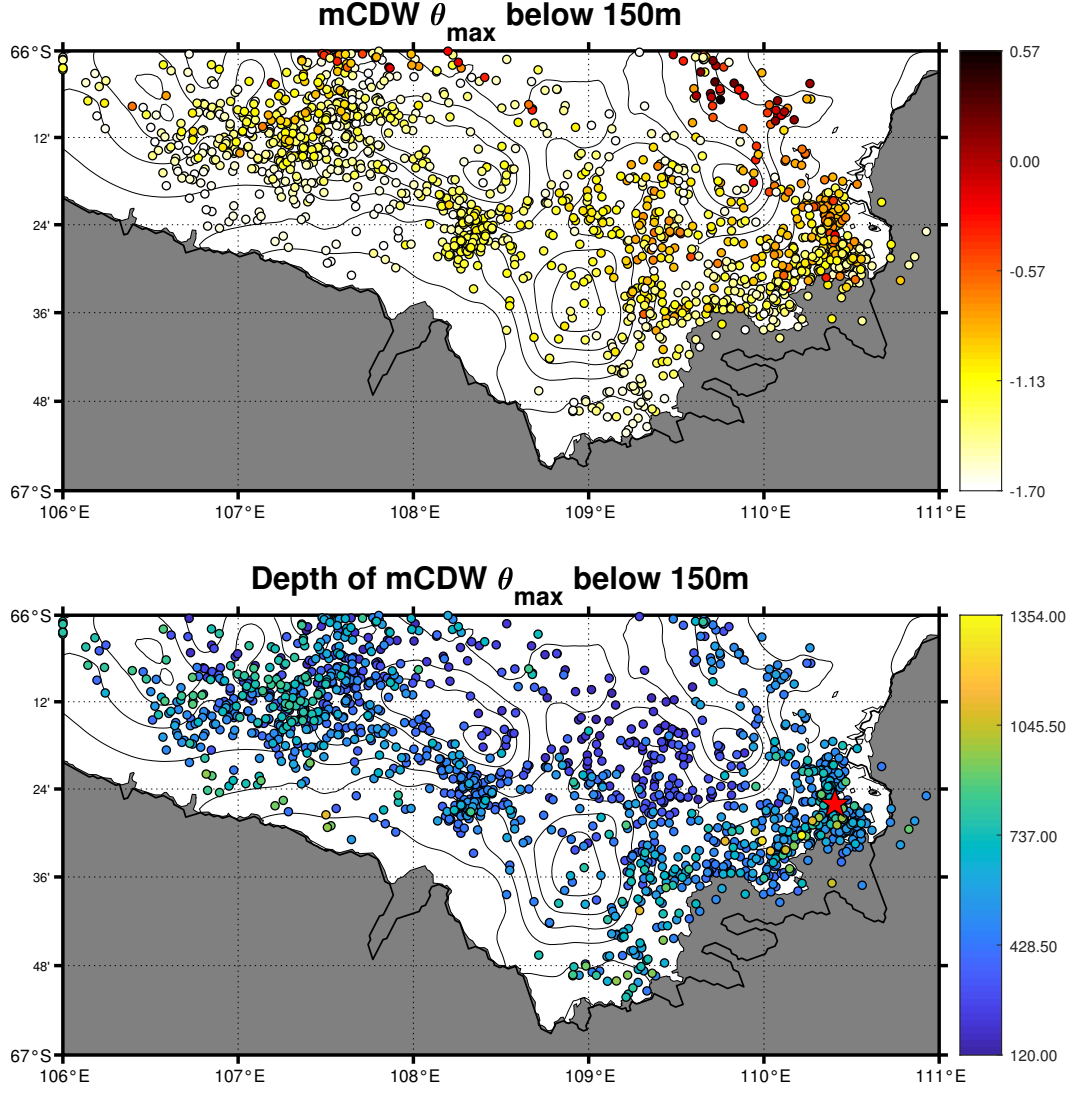


Figure 9. mCDW θ_{max} and depth of θ_{max} . Top panel shows maximum potential temperature of each mCDW profile in Vincennes Bay. Bottom panel indicates the depth where the maximum mCDW is found. A profile near the shelf that shows similar characteristics (θ and depth) to the one found near the Totten Ice Shelf is highlighted with a red star.

their surface height by almost 3 meters since 2008 (Viñas, 2018). Although small when compared to West Antarctica, the ice loss is indicative that East Antarctica might not be as sheltered from melting as previously thought and that its glaciers are already under ocean-driven change (Witze, 2018).

Exacerbating matters, the subglacial basins drained by Vincennes Bay’s glaciers are grounded below sea level (Viñas, 2018). Not much is known about the bathymetry in the area, but if the bedrock below the glaciers sloped downward inland of the grounding line as it does in the neighbouring Totten Glacier (Greenbaum et al., 2015), we may expect accelerated retreat of the glacier due to the Marine Ice Shelf Instability (Edwards et al., 2019). The maximum depth of the seal dives near the glaciers is up to 600 m deeper than indicated by BedMap2 bathymetry (Fretwell et al., 2013), indicating that warm mCDW has access to the ice-shelf cavity at depth, where it can drive rapid basal melt (Millan et al., 2020).

5 Conclusion

Many questions remain on the future of AABW production in Vincennes Bay, and also whether the Vanderford Polynya might be headed to a scenario where it doesn’t generate deep winter convection due to increased stratification of the ocean below. Silvano et al. (2017) showed that weak sea-ice production in Dalton Polynya results in increased stratification and impedes winter convection near the Totten Glacier, which allowed more mCDW intrusions on the shelf (Narayanan et al., 2019). From our observations in Vincennes Bay though, it seems mCDW intrusions are driving local glacial melt, which increases stratification making it harder for polynyas to generate deep convection. Convection to the sea floor in Vincennes Polynya only occurs at the end of a full winter’s worth of cooling and sea-ice formation. Additional freshwater input may be sufficient to make the Vincennes Bay system transition to a state similar to the Dalton Polynya/Totten continental shelf, with no DSW formation and enhanced inflow of warm mCDW driving additional glacial melt.

Given that intrusions of mCDW reaching the Vanderford Glacier can be much warmer than those observed at the Totten Glacier and that the local glaciers are already under basal melt, it is reasonable to assume Vincennes Bay’s polynyas could go the same way as the neighbouring Dalton. Vincennes Bay is a great example of an AABW source that is potentially nearing a tipping point at which it will stop forming bottom water. It only just manages to produce enough DSW to export into the top of the offshore AABW layer (Kitade et al., 2014). Further study and monitoring of this region will determine if and when enhanced-melting of the local glaciers will shut down this source completely. For now, this study shows evidence that the process is already underway.

Thanks to the contribution of instrumented seal CTD data from regions and seasons outside traditional ship-based measurements, there has been a series of novel oceanographic discoveries in Antarctic coastal regions. From our new observations of mCDW intrusions in Vincennes Bay, it is now important to elucidate if these intrusions have always been a part of the Antarctic system, previously overlooked because of sampling limitations or if this is a relatively new process that will continue to increase into the future. Although previously thought to be sheltered, both Vincennes and Totten continental shelves and ice fronts are reached by warm mCDW, showing that this part of East Antarctica is no longer isolated from warm water. Long-term observations of how, where and how often mCDW intrudes onto the East Antarctic continental shelf will be an important component of understanding how changes in Antarctic water mass structure and interactions will affect global climate.

Acknowledgments

This work was funded by University of Tasmania and supported by the French Polar Institute (program 109: PI. H. Weimerskirch and the SNO-MEMO and CNES-TOSCA) in collaboration with The Integrated Marine Observing System (IMOS). Australia's Integrated Marine Observing System (IMOS) is enabled by the National Collaborative Research Infrastructure Strategy (NCRIS). It is operated by a consortium of institutions as an unincorporated joint venture, with the University of Tasmania as Lead Agent. We would also like to thank the MEOP consortium and all scientists who participated in the data collection and processing, making it freely available. The dataset for this research can be found at the MEOP consortium website (www.meop.net) and is described in Treasure et al. (2017); Roquet et al. (2014, 2017).

References

- Bindoff, N. L., Rosenberg, M. A., & Warner, M. J. (1999). On the circulation and water masses over the antarctic continental slope and rise between 80 and 150°E [Journal Article]. *Deep Sea Research Part II: Topical Studies in Oceanography*, 47(12-13), 2299-2326.
- Bindoff, N. L., Williams, G. D., & Allison, I. (2001). Sea-ice growth and water-mass modification in the mertz glacier polynya, east antarctica, during winter [Journal Article]. *Annals of Glaciology*, 33, 399-406. doi: 10.3189/172756401781818185
- Charrassin, J., Roquet, F., Park, Y., Bailleul, F., Guinet, C., Meredith, M., ... Costa, D. (2010). New insights into southern ocean physical and biological processes revealed by instrumented elephant seals [Conference Proceedings]. In *Proceedings of oceanobs 09: Sustained ocean observations and information for society*. (Vol. 2). ESA Publication WPP-306. doi: 10.5270/OceanObs09.cwp.15
- Edwards, T. L., Brandon, M. A., Durand, G., Edwards, N. R., Golledge, N. R., Holden, P. B., ... Wernecke, A. (2019). Revisiting antarctic ice loss due to marine ice-cliff instability [Journal Article]. *Nature*, 566(7742), 58-64. doi: 10.1038/s41586-019-0901-4
- Foldvik, A., & Kvinge, T. (1974). Conditional instability of sea water at the freezing point [Conference Proceedings]. In *Deep sea research and oceanographic abstracts* (Vol. 21, p. 169-174). Elsevier.
- Fretwell, P., Pritchard, H. D., Vaughan, D. G., Bamber, J. L., Barrand, N. E., Bell, R., ... Zirizzotti, A. (2013). Bedmap2: improved ice bed, surface and thickness datasets for antarctica [Journal Article]. *The Cryosphere*, 7(1), 375-393. doi: 10.5194/tc-7-375-2013
- Gade, H. G. (1979). Melting of ice in sea water: A primitive model with application to the antarctic ice shelf and icebergs [Journal Article]. *Journal of Physical Oceanography*, 9(1), 189-198.
- Gill, A. (1973). Circulation and bottom water production in the weddell sea. *Deep Sea Research and Oceanographic Abstracts*, 20(2), 111 - 140. doi: [https://doi.org/10.1016/0011-7471\(73\)90048-X](https://doi.org/10.1016/0011-7471(73)90048-X)
- Greenbaum, J. S., Blankenship, D. D., Young, D. A., Richter, T. G., Roberts, J. L., Aitken, A. R. A., ... Siegert, M. J. (2015). Ocean access to a cavity beneath totten glacier in east antarctica [Journal Article]. *Nature Geoscience*, 8(4), 294-298. doi: 10.1038/ngeo2388
- Harcourt, R., Sequeira, A. M. M., Zhang, X., Roquet, F., Komatsu, K., Heupel, M., ... Fedak, M. A. (2019). Animal-borne telemetry: An integral component of the ocean observing toolkit [Journal Article]. *Frontiers in Marine Science*, 6(326). doi: 10.3389/fmars.2019.00326
- Herraiz-Borreguero, L., Coleman, R., Allison, I., Rintoul, S. R., Craven, M., & Williams, G. D. (2015). Circulation of modified circumpolar deep water

- and basal melt beneath the amery ice shelf, east antarctica [Journal Article].
Journal of Geophysical Research: Oceans, 120(4), 3098-3112.
- Jacobs, S. (1986). The antarctic slope front [Journal Article]. *Antarct. JUS*, 21(5), 123-124.
- Jacobs, S. (1991). On the nature and significance of the antarctic slope front [Journal Article]. *Marine Chemistry*, 35(1-4), 9-24.
- Jacobs, S. (2004). Bottom water production and its links with the thermohaline circulation [Journal Article]. *Antarctic Science*, 16(4), 427-437.
- Jacobs, S., Amos, A. F., & Bruchhausen, P. M. (1970). Ross sea oceanography and antarctic bottom water formation [Journal Article]. *Deep-Sea Research*, 17, 935-962.
- Jacobs, S., Jenkins, A., Giulivi, C. F., & Dutrieux, P. (2011). Stronger ocean circulation and increased melting under pine island glacier ice shelf [Journal Article]. *Nature Geoscience*, 4(8), 519-523. doi: 10.1038/ngeo1188
- Jonsen, I. D., Patterson, T. A., Costa, D. P., Doherty, P. D., Godley, B. J., Grecian, W. J., ... Robison, P. W. (2020). A continuous-time state-space model for rapid quality-control of argos locations from animal-borne tags [Journal Article]. *arXiv preprint arXiv:2005.00401*.
- Kitade, Y., Shimada, K., Tamura, T., Williams, G. D., Aoki, S., Fukamachi, Y., ... Ohshima, K. I. (2014). Antarctic bottom water production from the vincennes bay polynya, east antarctica [Journal Article]. *Geophysical Research Letters*, 41(10), 3528-3534. doi: 10.1002/2014gl059971
- Kusahara, K., Hasumi, H., & Tamura, T. (2010). Modeling sea ice production and dense shelf water formation in coastal polynyas around east antarctica [Journal Article]. *Journal of Geophysical Research: Oceans*, 115(C10).
- Liu, Y., Moore, J. C., Cheng, X., Gladstone, R. M., Bassis, J. N., Liu, H., ... Hui, F. (2015). Ocean-driven thinning enhances iceberg calving and retreat of antarctic ice shelves [Journal Article]. *Proceedings of the National Academy of Sciences*, 112(11), 3263-3268.
- Marshall, J., & Speer, K. (2012). Closure of the meridional overturning circulation through southern ocean upwelling [Journal Article]. *Nature Geoscience*, 5, 171. doi: 10.1038/ngeo1391
- Mensah, V., Roquet, F., Siegelman-Charbit, L., Picard, B., Pauthenet, E., & Guinet, C. (2018). A correction for the thermal mass-induced errors of ctd tags mounted on marine mammals [Journal Article]. *Journal of atmospheric and oceanic technology*, 35(6), 1237-1252.
- Millan, R., St-Laurent, P., Rignot, E., Morlighem, M., Mouginot, J., & Scheuchl, B. (2020). Constraining an ocean model under getz ice shelf, antarctica, using a gravity-derived bathymetry [Journal Article]. *Geophysical Research Letters*, 47(13), e2019GL086522.
- Morrison, A., Hogg, A. M., England, M., & Spence, P. (2020). Warm circumpolar deep water transport toward antarctica driven by local dense water export in canyons [Journal Article]. *Science Advances*, 6(18), eaav2516.
- Narayanan, A., Gille, S. T., Mazloff, M. R., & Murali, K. (2019). Water mass characteristics of the antarctic margins and the production and seasonality of dense shelf water [Journal Article]. *Journal of Geophysical Research: Oceans*, 124(12), 9277-9294. doi: 10.1029/2018jc014907
- Ohshima, K. I., Fukamachi, Y., Williams, G. D., Nihashi, S., Roquet, F., Kitade, Y., ... Wakatsuchi, M. (2013). Antarctic bottom water production by intense sea-ice formation in the cape darnley polynya [Journal Article]. *Nature Geoscience*, 6(3), 235-240. doi: 10.1038/ngeo1738
- Rignot, E., Jacobs, S., Mouginot, J., & Scheuchl, B. (2013). Ice-shelf melting around antarctica [Journal Article]. *Science*, 341(6143), 266-270.
- Rintoul, S. R. (1985). On the origin and influence of adélie land bottom water [Journal Article]. *Ocean, ice, and atmosphere: Interactions at the Antarctic conti-*

- 563 *mental margin*, 75, 151-171.
- 564 Rintoul, S. R., Silvano, A., Pena-Molino, B., van Wijk, E., Rosenberg, M., Green-
565 baum, J. S., & Blankenship, D. D. (2016). Ocean heat drives rapid basal melt
566 of the totten ice shelf [Journal Article]. *Science Advances*, 2(12), e1601610.
- 567 Roquet, F., Boehme, L., Block, B., Charrassin, J. B., Costa, D., Guinet, C., ...
568 McMahon, C. R. (2017). Ocean observations using tagged animals [Journal
569 Article]. *Oceanography*.
- 570 Roquet, F., Williams, G., Hindell, M. A., Harcourt, R., McMahon, C., Guinet, C.,
571 ... Lovell, P. (2014). A southern indian ocean database of hydrographic pro-
572 files obtained with instrumented elephant seals [Journal Article]. *Scientific*
573 *data*, 1, 140028.
- 574 Schlosser, P., Bönisch, G., Rhein, M., & Bayer, R. (1991). Reduction of deepwater
575 formation in the greenland sea during the 1980s: Evidence from tracer data
576 [Journal Article]. *Science*, 251(4997), 1054-1056.
- 577 Siegelman, L., Roquet, F., Mensah, V., Rivière, P., Pauthenet, , Picard, B., &
578 Guinet, C. (2019). Correction and accuracy of high-and low-resolution ctd
579 data from animal-borne instruments [Journal Article]. *Journal of Atmospheric*
580 *and Oceanic Technology*, 36(5), 745-760.
- 581 Silvano, A., Rintoul, S., & Herraiz-Borreguero, L. (2016). Ocean-ice shelf interac-
582 tion in east antarctica [Journal Article]. *Oceanography*, 29(4), 130-143. doi: 10
583 .5670/oceanog.2016.105
- 584 Silvano, A., Rintoul, S. R., Peña-Molino, B., Hobbs, W. R., van Wijk, E., Aoki, S.,
585 ... Williams, G. D. (2018). Freshening by glacial meltwater enhances melt-
586 ing of ice shelves and reduces formation of antarctic bottom water [Journal
587 Article]. *Science advances*, 4(4), eaap9467.
- 588 Silvano, A., Rintoul, S. R., Peña-Molino, B., & Williams, G. D. (2017). Distribu-
589 tion of water masses and meltwater on the continental shelf near the totten
590 and moscow university ice shelves [Journal Article]. *Journal of Geophysical*
591 *Research: Oceans*, 122(3), 2050-2068. doi: doi:10.1002/2016JC012115
- 592 Treasure, A. M., Roquet, F., Ansorge, I. J., Bester, M. N., Boehme, L., Bornemann,
593 H., ... Fedak, M. A. (2017). Marine mammals exploring the oceans pole to
594 pole: a review of the meop consortium [Journal Article]. *Oceanography*, 30(2),
595 132-138.
- 596 Velicogna, I., Sutterley, T. C., & vanden Broeke, M. R. (2014). Regional acceleration
597 in ice mass loss from greenland and antarctica using grace time-variable grav-
598 ity data [Journal Article]. *Geophysical Research Letters*, 41(22), 8130-8137.
599 doi: 10.1002/2014gl061052
- 600 Viñas, M.-J. (2018). *More glaciers in east antarctica are waking up* [Web Page].
601 NASA's Earth Science News Team. Retrieved from [https://climate.nasa](https://climate.nasa.gov/news/2832/more-glaciers-in-east-antarctica-are-waking-up/)
602 [.gov/news/2832/more-glaciers-in-east-antarctica-are-waking-up/](https://climate.nasa.gov/news/2832/more-glaciers-in-east-antarctica-are-waking-up/)
- 603 Williams, G., Aoki, S., Jacobs, S., Rintoul, S., Tamura, T., & Bindoff, N. (2010).
604 Antarctic bottom water from the adélie and george v land coast, east antarc-
605 tica (140–149 e) [Journal Article]. *Journal of Geophysical Research: Oceans*,
606 115(C4).
- 607 Williams, G., & Bindoff, N. (2003). Wintertime oceanography of the adélie depres-
608 sion [Journal Article]. *Deep Sea Research Part II: Topical Studies in Oceanog-*
609 *raphy*, 50(8-9), 1373-1392.
- 610 Williams, G., Bindoff, N. L., Marsland, S. J., & Rintoul, S. R. (2008). Formation
611 and export of dense shelf water from the adélie depression, east antarctica
612 [Journal Article]. *Journal of Geophysical Research: Oceans*, 113(C4).
- 613 Williams, G., Herraiz-Borreguero, L., Roquet, F., Tamura, T., Ohshima, K. I., Fuka-
614 machi, Y., ... Hindell, M. (2016). The suppression of antarctic bottom water
615 formation by melting ice shelves in prydz bay [Journal Article]. *Nat Commun*,
616 7, 12577. doi: 10.1038/ncomms12577
- 617 Witze, A. (2018). *East antarctica is losing ice faster than anyone thought* [Web

618 Page]. Nature communications. Retrieved from [https://www.nature.com/](https://www.nature.com/articles/d41586-018-07714-1)
619 [articles/d41586-018-07714-1](https://www.nature.com/articles/d41586-018-07714-1)